BioMEMS to bionanotechnology: state of the art in integrated biochips and future prospects

Amit Gupta, H. Li, Rafael Gomez, W.-J. Chang, Y. M. Koo, et al.

Amit Gupta, H. Li, Rafael Gomez, W.-J. Chang, Y. M. Koo, H. Chang, G. Andreadakis, Demir Akin, Rashid Bashir, "BioMEMS to bionanotechnology: state of the art in integrated biochips and future prospects," Proc. SPIE 5593, Nanosensing: Materials and Devices, (29 December 2004); doi: 10.1117/12.580407

SPIE.

Event: Optics East, 2004, Philadelphia, Pennsylvania, United States

BioMEMS to bionanotechnology: state-of-the-art in integrated biochips and future prospects

A. Gupta[a], H. Li[a], R. Gomez[c], W-J Chang[d], Y. M. Koo[d], H. Chang[a], G. Andreadakis[a], D. Akin[a], R. Bashir[↑a,b],
[a]School of Electrical and Computer Engineering, [b]Department of Biomedical Engineering,
Purdue University, IN. USA., [c]Now with Department of Applied Physics, Caltech, Pasadena, CA.USA.,
[d]Department of Biological Engineering, Inha University, Korea

ABSTRACT

Biomedical or Biological Micro-Electro-Mechanical- Systems (BioMEMS) have in recent years become increasingly prevalent and have found widespread use in a wide variety of applications such as diagnostics, therapeutics and tissue engineering. This paper reviews the interdisciplinary work performed in our group in recent years to develop micro-integrated devices to characterize biological entities. We present the use of electrical and mechanically based phenomena to perform characterization and various functions needed for integrated biochips. One sub-system takes advantage of the dielectrophoretic effect to sort and concentrate bacterial cells and viruses within a micro-fluidic biochip. Another sub-system measures impedance changes produced by the metabolic activity of bacterial cells to determine their viability. A third sub-system is used to detect the mass of viruses as they bind to micro-mechanical sensors. The last sub-system described has been used to detect the charge on DNA molecules as it translocates through nanopore channels. These devices with an electronic or mechanical signal output can be very useful in producing practical systems for rapid detection and characterization of cells for a wide variety of applications in the food safety and health diagnostics industries. The paper will also briefly discuss future prospects of BioMEMS and its possible impact and on bionanotechnology.

Keywords: BioMEMS, Integrated Biochips, Bionanotechnology, Lab-on-a-chip, Microorganisms, Dielectrophoresis, Micromechanical Sensors, Nanopore, DNA

1. INTRODUCTION

Biomedical or Biological Micro-Electro-Mechanical Systems (BioMEMS) are at present a heavily researched area with a wide variety of important biomedical applications[1]. The ability to fabricate micro and nano-structures with scales and dimensions similar to biological entities has paved the way to new concepts and systems for a variety of cellular, diagnostic and therapeutic applications, such as intelligent biochips and biosensors[2,3]. There has also been the realization that life sciences could provide novel ideas and schemes that can contribute to the advancement of micro- and nanoscale physical systems. Figure 1 shows a schematic drawing of the key segments of research areas resulting from integration of life sciences and biomedical disciplines with micro- and nano-scale systems[4]. The areas on the right are applications of biology to micro- and nano-scale electronic systems and materials, while the areas on the left are applications of micro- and nano-scale systems to biological and biomedical problems.

One area of research that has become increasingly important is the handling, manipulation, and characterization of single cells and microorganisms using bioMEMS. The goal of such an effort should be to handle, detect, and characterize a single cell or microorganism; and micro-devices are ideally suited for such studies. In addition, reducing the time-to-result to be able to perform 'point-of-use' analysis is also necessary, and detection of single cells is vital to achieving this goal. Such endeavors can not only yield very important scientific results but can also be used immediately in practical diagnostic applications in the health and food industry, and in biological and chemical hazard prevention systems. This paper will present an overview of the interdisciplinary work that has been done by our group in recent years to develop components and sub-systems of an integrated biochip for detection and characterization of cells and microorganisms. As shown in figure 2, such a system should be able to perform all functions needed for rapid detection such as cell sorting, cell concentration, and cell detection. The cell detection module can actually include many functions such as cell lysing, DNA or protein detection, or whole cell detection using an antibody-based immunoassay approach.

↑ bashir@ecn.purdue.edu; phone 765-496-6229; fax 765-494-6441; https://engineering.purdue.edu/LIBNA

Nanosensing: Materials and Devices, edited by M. Saif Islam, Achyut K. Dutta,
Proceedings of SPIE Vol. 5593 (SPIE, Bellingham, WA, 2004)
0277-786X/04/$15 · doi: 10.1117/12.580407

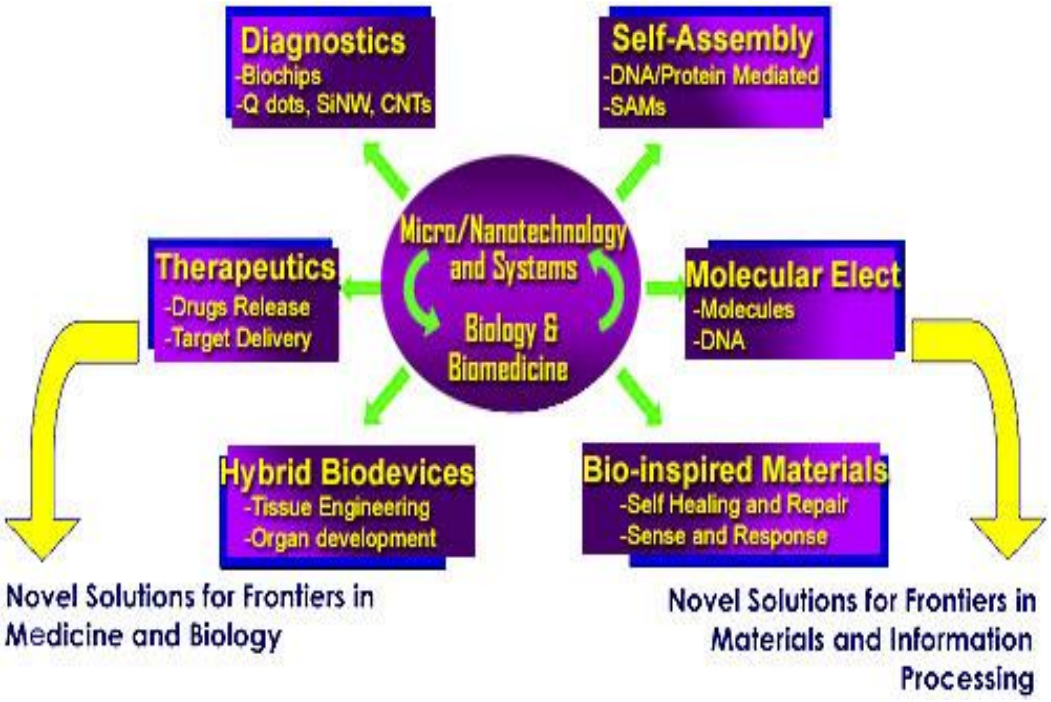

Fig. 1. Research area resulting from the integration of micro- and nanoscale systems with biomedical sciences (Ref. [4]).

Figure 2: The functions needed in an integrated biochip for rapid cell detection

2. CELL CONCENTRATION USING DIELECTROPHORESIS ON A CHIP

2.1. Background

The technique of dielectrophoresis (DEP) and manipulation of biological particles by electrical forces provide unique means to control the separation dynamics of biological agents. The method has numerous biological and medical

applications, e.g., identification and characterization of individual cells, purification of cell subpopulations from mixture suspension, etc.

Dielectrophoretic forces occur on cells when a non-uniform AC electrical field interacts with field-induced electrical polarization[5]. The time-averaged dielectrophoretic force F for a dielectric sphere immersed in a medium is represented as,

$$F = 2\pi\varepsilon_0\varepsilon_m r^3 \,\mathrm{Re}\,[f_{CM}]\nabla|E_{RMS}|^2 \tag{1}$$

where ε_o is the vacuum dielectric constant, r is the particle radius, E_{RMS} is the root mean square value of the electric field, and f_{CM} is known as the Clausius-Mossotti factor, defined as:

$$f_{CM} = \frac{\varepsilon_p - \varepsilon_m}{\varepsilon_p + 2\varepsilon_m} \tag{2}$$

where ε_p and ε_m are the relative complex permittivities of the particle and the medium respectively. When the dielectric constant of particle is larger than that of medium, i.e., $\mathrm{Re}[f_{CM}] > 0$, the DEP is called positive and the particle moves towards the locations with the greatest electric field gradient. Whereas the dielectric constant of particle is smaller than that of medium, i.e., $\mathrm{Re}[f_{CM}] < 0$, the DEP is called negative and particle moves to the locations with smallest electric field gradient. Since the dielectric properties of different species of particles are different and the dielectric constants of both particle and medium are functions of frequency, $\mathrm{Re}[f_{CM}]$ may have different signs for different species of particles at a given frequency. By choosing a proper frequency and a suspending medium so that two different particles with different dielectric properties may experience positive and negative DEP respectively, particles can be sorted and separated. Electric field gradients can be readily achieved on a chip using two-dimensional electrodes.

Biological entities such as cells, proteins and DNA consist of adjacent structures of materials that have very different electrical properties and exhibit large induced boundary polarizations that are highly dependent on the applied field frequency as well as their physiological states. Upon death, the cell membrane becomes permeable and its conductivity can increase by a factor of 10^4 due to the cell contents exchanging material freely with the external medium through the small pores on the membrane. This large change in the dielectric properties on cell death indicates a large change in the dielectric polarizability. Hence a large difference in DEP responses (positive and negative respectively) and a selective separation can be achieved between live and dead cells.

2.2. Separation and Concentration of Cells in a Chip

During previous studies, our group was able to achieve the dielectrophoretic separation of live and heat-killed *Listeria innocua* cells[6]. It was observed that the dielectrophoretic behaviors of live and dead cells differed in the frequency range from ~30KHz to ~100KHz in the selected medium (water). Both live and dead cells can collect either on the top centers of the electrodes in negative dielectrophoresis [Figure 3(a)] with a 10KHz signal. The cells separate in positive dielectrophoresis for the electric field configuration of the interdigitated microelectrodes used in our experiments with 50KHz signal [Figure 3(b)]. The viability of the cells was verified by a rapid epifluorescence staining method using the LIVE/DEAD Bacterial Viability Kit (BacLight, Molecular Probes, Eugene, OR) and the live and dead cells can be monitored simultaneously in the experiments. It is envisioned that the separation and manipulation of microorganisms and viruses on biochips using dielectrophoresis will become a very useful method in sample preparation and preprocessing and in diagnostic applications.

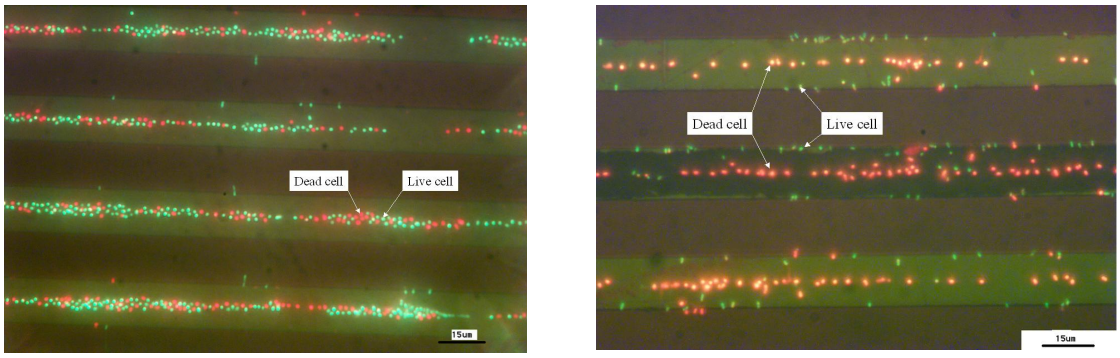

(a) (b)

Figure 3: Top view optical pictures of cells on 15μm line/space interdigitated electrodes, (a) Negative dielectrophoresis for both live and heat-treated *Listeria innocua* cells by applying. Cells collect on the top centers of the electrodes. (b) Dielectrophoretic separation of live and heat-treated *Listeria*. Most live cells (green) collect on the edges of the electrodes, whilst the heat-treated cells (red) collect on the top centers of the electrodes (Ref. [6]).

Dielectrophoresis can also be used to selectively capture a particle of interest inside the chip using a dielectrophoretic filter[7]. Polystyrene beads (coated with antibodies selective to target species) are flowed through the chip. An array of electrodes is used to generate an AC electric field at a frequency on the order of 1 MHz. When the beads approach the electrodes, they will experience a dielectrophoretic force which repels them away from regions where the gradient of the electric field is maximum (at the edges of the electrodes). If this force is equal to or larger than the drag force exerted on the beads by the liquid flow, the beads remain trapped in the chamber (along with the bacterial cells they carry) while everything else in the sample flows out of the chip. Figure 4(a) shows beads flowing freely through the chip while the electric field is off; Figure 4(b) shows the beads accumulating in the middle of the electrodes when the field is turned on (the beads cannot cross the edges of the electrodes, where the dielectrophoretic force is maximum).

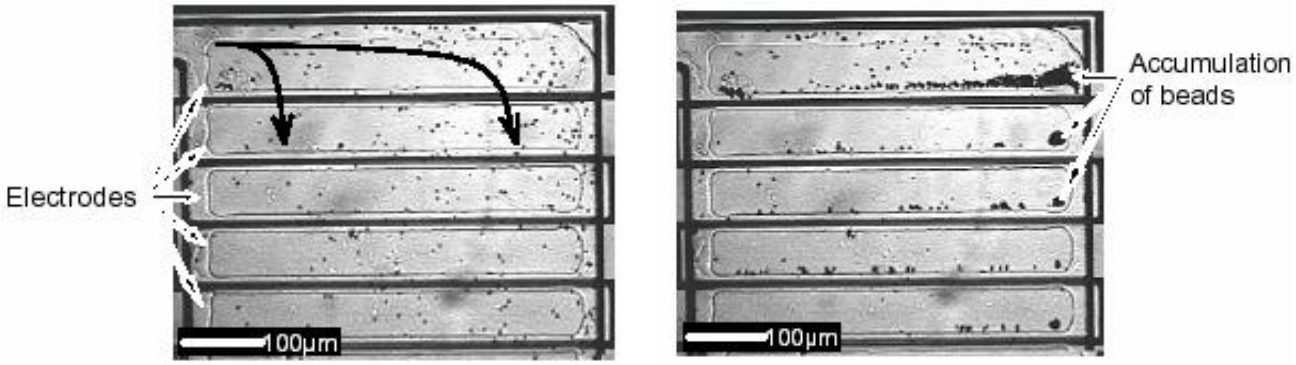

(a) (b)

Figure 4. Dielectrophoretic capture of particles in a fluid flow. (a) Beads with bacteria flowing through the chip while the ac electric field is off. The two curved arrows indicate approximate flow lines. (b) Beads captured at the center of the electrodes when the field is turned on, with the carrier fluid (water) still flowing through (Ref. [7]).

2.3 Real time virus fluorescent imaging and dielectrophoretic trapping

Dynamic visualization of interactions of nanometer scale biological molecules with and in micro/nano-electro-mechanical systems and micro-fluidic bio-chips are limited by the lack of imaging tools and visualization techniques. Due to their nanometer size dimensions, we have been unable to visually confirm the efficiency of real-time separation of these virus particles in chip-based devices with dielectrophoretic traps and in gravimetric biosensors by optical means; hence, a method to see these biological entities was essential. We have developed fluorescence labeling and visualization

techniques that allow the direct visualization of single particles in micro-fluidic devices[8]. We are working with vaccinia virus, which is a member of the poxvirus family, whose members characteristically have a large DNA genome and replicate in the cytoplasmic compartment of the cell. The viral envelope and the proteins were stained with lipophilic stain DiOC6(3) (Molecular Probes, Eugene, OR) and viral DNA was labeled with nucleophilic stain Hoechst dye or YOYO-1 (molecular Probes). Briefly, the suspension containing virus particles were incubated with a mixture of DiOC6(3), 1μM final concentration, and either Hoechst dye or YOYO-1 (μM final concentrations) and incubated at room temperature for 20 minutes after which they were subjected to 20,000g centrifugation for 10 minutes. The viral pellets were rinsed three times by resuspending in distilled-water and centrifugation as above. Final virus pellets were resuspended in distilled-water until being used in the experiments. Figure 5 shows the fluorescent pictures of the particles clearly showing the staining of viral capsid (green, outer) and the DNA (blue, inner).

A dielectrophoretic filter was then constructed in a micro-fluidic biochip. KOH was used to etch a chamber of 12μm deep and 350μm wide into single crystal silicon substrate. After a thermal oxidation, a metal (Ti/Pt) pattern of interdigitated electrode array was sputtered and defined at the bottom of the chamber. Another plasma enhanced oxide was deposited and fluid inlet and outlet micro-tubes were inserted into the ports etched by Deep Reactive Ion Etch (DRIE) to the two ends of the chamber. The top of the chamber was covered with a glass slide by anodic bonding. In the experiment, virus sample solution in distilled-water (conductivity 1.5μS/cm) was injected into the chamber using a syringe pump (World Precision Instruments Inc., SP200i) and a 250μl gas-tight luer-lock syringe (ILS250TLL, World Precision Instruments Inc.). The flow rate was set to be at 0.1μl/min and precautions were taken to avoid bubbles. The virus particles experienced positive dielectrophoresis and were collected at the electrode edges with a sine wave excitation at 1MHz and ~7V_{pp} (into 50Ω) generated by an HP 33120A signal generator. Figure 6(a) shows a cross-section of the device along with images of captured viruses. The viruses experienced positive DEP (in DI water and air), i.e. they get captured at the edges of the electrodes in the regions of high field gradient.

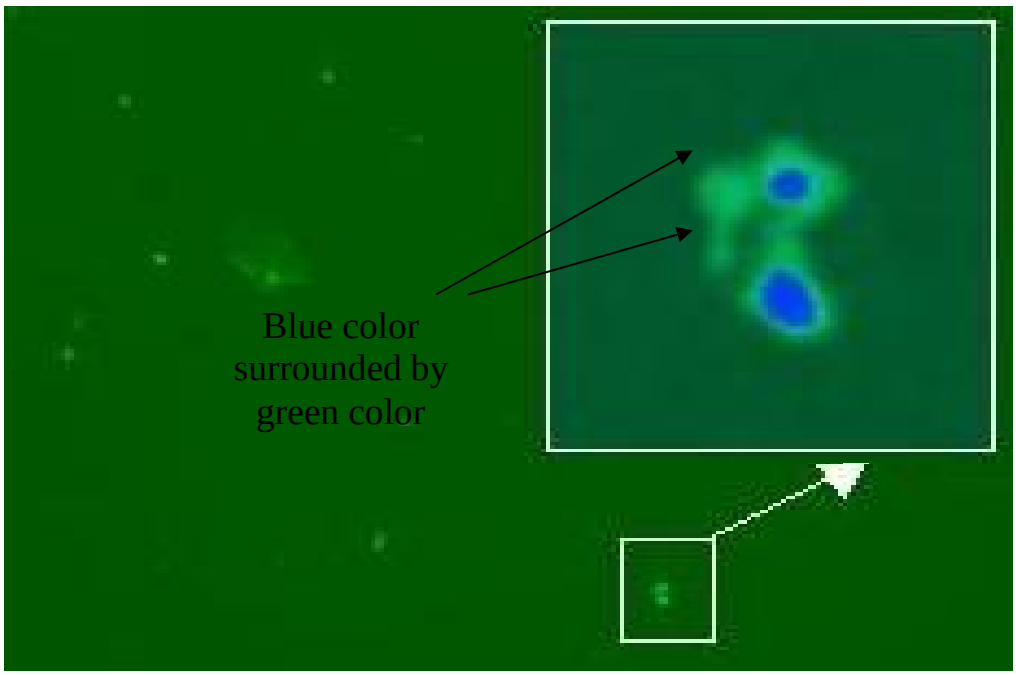

Figure 5: Dual-labeled viruses where the viral nucleic acids were stained blue due to penetration and intercalation of nucleophilic dye within the green-labeled viral capsids due to lipohilic dye (Ref. [8]).

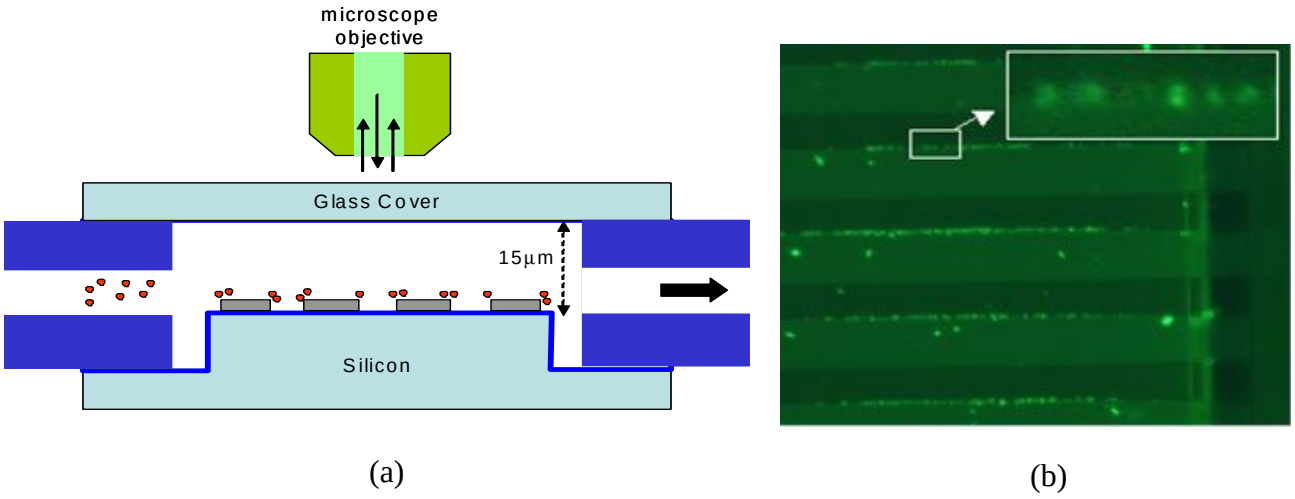

Figure 6. Dielectrophoretic capture and epi-fluorescence microscopic visualization of vaccinia virus particles. (a) Cross-sectional schematic diagram of the micro-fluidic device. (c) Top view of labeled vaccinia virus particles trapped at the edges of the electrode and visualized though a FITC filter (Ref. [8]).

The techniques above can be used to concentrate bacteria, cells, viruses, DNA, or proteins, as long as their dielectric constant is different than the dielectric constant of the medium that they are suspended in. Hence, this technique can be used to separate virus particles from other particles in air, or used to concentrate particles of a particular type in a micro-chamber of interest. In the following section, a sub-system will be described that makes use of dielectrophoretic filters in order to trap and concentrate bacterial cells to enhance and speed-up the detection capability of the chip.

3. MICRO-SCALE BACTERIAL CELL CULTURE IN A CHIP

3.1 Device Fabrication

The metabolic activity of viable microorganisms changes the ionic concentration of the medium in which they are suspended, by the secretion of ionic metabolic byproducts. This change can be detected by measuring the AC impedance of metallic electrodes in contact with the medium[9]. We have designed a silicon-based biochip based on this concept, which will be used for rapid detection of live or viable microorganisms in food samples. Large scale systems for impedance-based detection of bacterial metabolism have been in use for a long time, but this is the first attempt at miniaturizing this assay[10]. By confining a few bacterial cells into volumes on the order of nanoliters, the sensitivity and speed of the assay can be greatly improved. The device consists of a network of channels and chambers etched in a crystalline silicon substrate as shown in figure 7. Fluidic input/output ports are formed by reactive ion etching of deep trenches in the substrate that are connected to the channels and chambers. Micro-bore tubes are inserted in these trenches to bring fluids in and out of the device. A glass cover is bonded on top of the device, with a spin-on-glass adhesion layer, to create a fully sealed micro-fluidic system. Electronic detection is done by interdigitated platinum electrodes patterned on the bottom of the analysis chambers. Figure 8 shows an optical micrograph of a hybrid PDMS/Silicon Biochip[11]. PDMS cover was made using Teflon tubing and hole-punch without photolithographic method. The cover was made of two layers of PDMS. As a first layer, mixture of PDMS and curing agent was poured onto the 3" silicon wafer with the thickness of 500 µm. The 3" wafer was first silanized with trichloro(3,3,3-trifluoropropyl) silane to prevent the bonding of cured PDMS. For three-dimensional micro-channel, Teflon tubing (Cole Parmer Co.) that has 360 µm OD and 50 µm ID was cut into 7 mm long pieces, and put between two layers of PDMS. Cured PDMS cover embedding Teflon tubing was peeled off from the mold, and cut into the adequate size for silicon biochip. The size of silicon biochip was 9.12 mm x 8.9 mm. Detailed dimensions and fabrication methods for silicon base are same as described above. The Teflon tubing was pulled out of PDMS cover and holes for output-flow of liquid were punched from the both faces of cover, after one open end of horizontal channel was blocked with PDMS. The hole for input-flow was punched after aligned on the silicon biochip.

3.2 Results

Preliminary experiments with the biochip were performed using the non-pathogenic microorganism *Listeria innocua*. This bacterium is a close relative of *Listeria monocytogenes*, which is a well known pathogen that can cause severe infections and even death in immuno-compromised individuals. The bacteria were suspended in a low conductivity buffer, incubated off-chip at 37ºC for 2 hours, and injected into a 5.3nl chamber in the biochip. The impedance of the suspensions and of plain buffer (without bacteria) was measured at frequencies between 100Hz and 1MHz. The measured complex impedance as a function of frequency was fitted to a simple circuit model[11]. The model consisted of two constant-angle interfacial impedances of magnitude $1/B$, in series with a resistance R_s, plus a dielectric capacitance C_{di} in parallel with the other components. Figure 9 shows the normalized differences in the total impedance at 11.43kHz (Z), the resistance R_s, and the interface parameter B, extracted from the bacterial suspensions, with respect to the values obtained from plain buffer. These measurements indicated that the metabolic activity of a minimum of 50 to 200 cells can be detected. The device is currently being redesigned to increase its sensitivity to analyze a single cell.

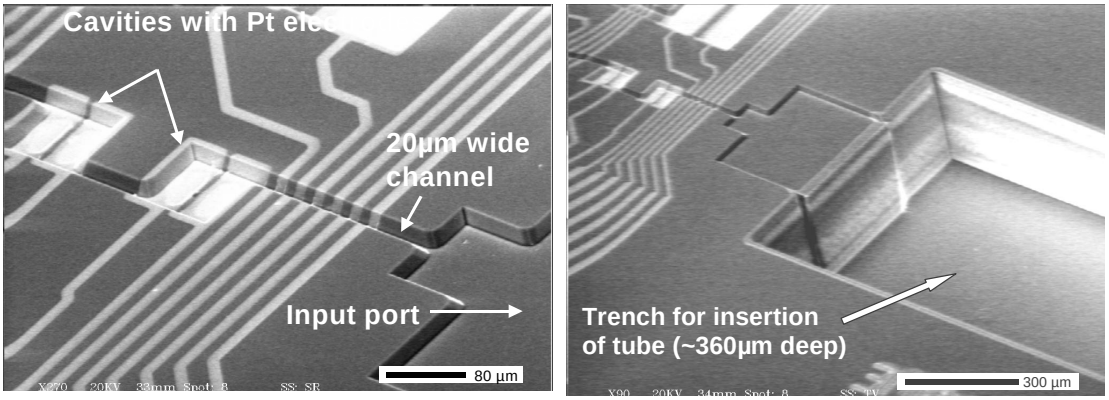

(a) (b)

Fig. 7: (a) Electron microscope pictures of the channels and wells in the biochip, (b) Close up of the fluidic I/O port in the biochip (Ref. [10]).

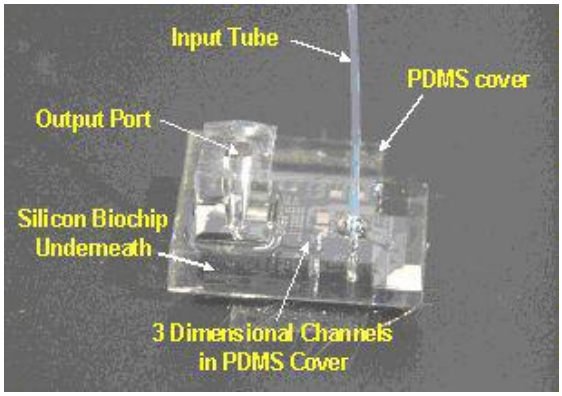

Figure 8: An optical micrograph of the hybrid PDMS/silicon micro-fluidic biochip (Ref. [11]).

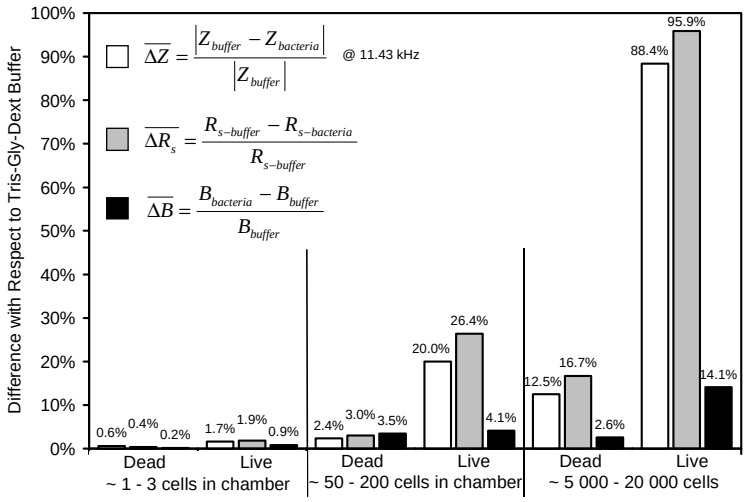

Fig. 9: Normalized differences between the bacterial suspensions and plain buffer (without bacteria) for three impedance-derived parameters (Ref. [10]).

4. MICRO/NANOMECHANICAL BIOSENSORS

4.1 Background

Micro- and nano-scale mechanical sensors have been shown to be extremely sensitive biosensors. The change in resonant frequency of silicon based cantilever beams, due to mass change after antigen binding can be used as the detection scheme. This technique has been previously demonstrated with the capability to fundamentally detect single bacterial cells[12]. The change in mass at the free end of the cantilever in relation to a change in resonant frequency can be given as,

$$\Delta m = \frac{k}{4n\pi^2}\left(\frac{1}{f_1^2} - \frac{1}{f_o^2}\right), \tag{3}$$

where, k is the spring constant of the cantilever beam, f_0 is the initial resonant frequency before the addition of the mass, f_1 is the resonant frequency after the mass addition; and n = 1 in the case when the added mass is placed right at the free end and n~0.24 when the additional mass is uniformly distributed over a rectangular shaped cantilever beam.

4.2 Experimental Results

We have recently reported the demonstration of a nanoscale thick cantilever beam operating as a mass detector, with a sensitivity of the mass of a single vaccinia virus particle[13]. In general, decreasing the overall dimensions of the cantilever beams results in a corresponding increase in their mass sensitivity. In previous works on the detection of virus particles, macroscale quartz crystal micro-balance devices requiring an external power supply were used and the detachment of virus particles were measured[14]. In our experiments, we have used nanomechanical devices on a chip, with the measurement set-up sensitive enough to measure thermal and ambient noise induced deflections and thus not requiring an external source to excite the cantilever beams.

The process flow for the fabrication of the cantilever beam has been described in detail elsewhere[13]. The measurement of the cantilever resonant frequency was performed using a microscope scanning laser Doppler vibrometer (MSV-300 from Polytec PI) with a laser beam spot size of around 1-2um. The resonant frequencies of typical cantilever beams of length around 5 μm, width around 1.5 μm, and thickness around 30 nm, was in the 1-2 MHz range with quality factor of around 5-7. The cantilevers beams were first cleaned in a solution of (H_2O_2:H_2SO_4=1:1), rinsed in DI water, immersed in ethanol and dried using a critical point drier (CPD). The frequency spectrum was then measured in order to obtain the 'unloaded' resonant frequencies of the cantilever beams. Next, purified vaccinia virus particles at a concentration of *ca.*

10^9 PFU/ml in DI water were introduced over the cantilever beams and allowed to interact for 30 min, following which the cantilever beams were rinsed in ethanol and dried using CPD. The resonant frequency of the cantilever beams were then measured again in order to obtain the 'loaded' resonant frequencies. Using the mechanics of a spring-mass system described by equation 3 (with n=1), we were able to determine the added mass for the corresponding change in resonant frequency. The cantilever beams were calibrated by obtaining their spring constant, k, using the unloaded resonant frequency measurement f_0, quality factor Q, and the plan dimensions (length and width) of the cantilever beam[15]. The resonant frequency and the quality factor were obtained by fitting the vibration spectra data to the amplitude response of a simple harmonic oscillator (SHO). The measured spring constant of the cantilever beams was around 0.005-0.01 N/m. The virus particles were counted by observing the cantilever beams and virus particles using a scanning electron microscope (SEM). The effective mass contribution of the viruses was calculated based on their relative position from the fixed end of the cantilever beams. Using the measurements from the various cantilever beams, we plotted the resonant frequency shift (decrease) versus the effective number of virus particles that were observed on the cantilever beam, as shown in Fig. 10(a). The relationship was linear, as expected, clearly proving the validity of the measurements. Fig. 10(b) shows the resonant frequency shift (Δf = 60 kHz) after the addition of a single virus particle. We measured an average dry mass of 9.5 fg for a single vaccinia virus particle, which is in the range of the expected mass of 5-8 fg[16]. The measured mass sensitivity of the present cantilever beams for a 1 kHz frequency shift is 160 ag added mass (6.3 Hz/ag).

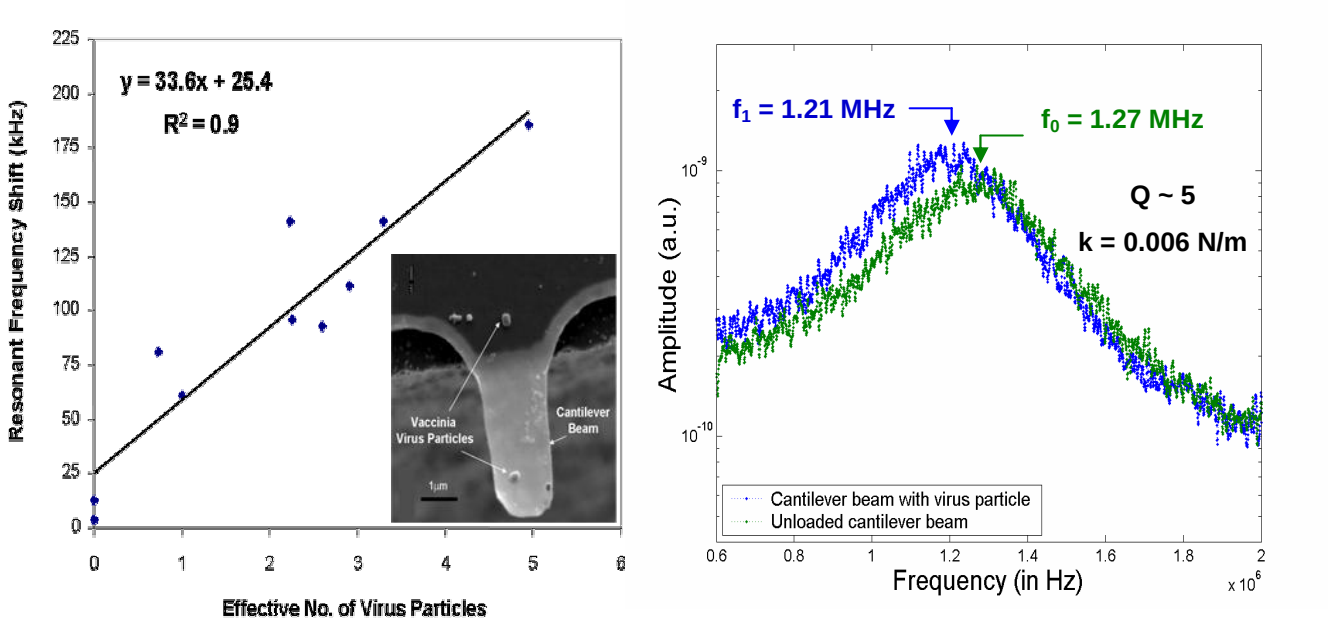

(a) (b)

Fig. 10 (a) Plot of measured resonant frequency shift (decrease) versus the effective number of virus particles on the cantilever beams. A linear fit was performed on the data points. Inset shows an SEM of a cantilever beam with a single vaccinia virus particle. (b) Plot of resonant frequency shift after loading of a single virus particle. There is a 60 kHz decrease in the resonant frequency of the cantilever beam. The unloaded resonant frequency is f_0 = 1.27 MHz, quality factor Q = 5, and spring constant k = 0.006 N/m. The resonant frequencies were obtained from a fitting the amplitude response of a simple harmonic oscillator to the measured data (Ref. [13]).

There is ongoing work in our group to functionalize the surface of the cantilever beams with antibodies in order to be able to specifically detect the target antigens. Future work will involve incorporating on-chip dielectrophoresis filters that have been described in the previous sections in order to concentrate the target analytes from air.

5. DNA CHARGE DETECTION BASED ON IONIC CURRENT FLUCTUATIONS USING NANOPORE CHANNELS

5.1 Background

The sub-systems and devices that have been described so far in this paper have been designed to interact with whole, intact cells. It may become necessary in an integrated biochip to have the ability to analyze the constituents of a cell such as DNA, proteins, mRNA and other biochemical molecules. Hence, our group has pursued the study of single molecule sensors such as the nanopore. Nanoscale pores within biological or artificial membranes acting as mechanical gating elements are very promising devices as single molecule sensors for the rapid characterization and sequencing of nucleic acid molecules. The two terminal electrical measurements of translocation of polymers through single ion channels[17] and that of ssDNA molecules through protein channels[18] have been demonstrated, and have sparked tremendous interest in such single molecule sensors.

The electronic signature of dsDNA moving through these nanopores can be quite complex and the conformational changes in the molecule cannot be ignored[19]. 'Channels' with nanoscale diameters have been shown to be one method to suppress signatures due to conformational changes by increasing the entropic energy barrier for molecules to enter the nanopore[20]. The prevailing view regarding the nanopore sensors is that there exists no electrical interaction between the nanopore and the translocating molecule, and that all nanopore sensors reported to-date, whether biological or artificial, operate as a Coulter-counter, i.e. the ionic current measured across the pore decreases (is mechanically blocked) when the DNA molecule transverses through the pore. We have fabricated nanopore 'channel' sensors with a silicon oxide inner surface and our results challenge the prevailing view of exclusive mechanical interaction during the translocation of dsDNA molecules through these channels. We demonstrate that the ionic current can actually increase due to electrical gating of surface current in the channel due to the charge on the DNA itself.

5.2 Results

We fabricated 50-60nm long, 4-5nm diameter nanopore channels in micro-machined silicon membranes[21]. The nano-pore channels were fabricated with a process similar to one described earlier[22] and commenced with double polished SOI wafers[21]. The buried oxide and SOI layers were 400 nm and 190 nm thick, respectively. A 100 nm thermal oxide was grown on the SOI wafer. An LPCVD nitride layer was deposited and etch windows (~670 μm by 670 μm area) were formed on the backside. The nitride and oxide was etched and the handle layer of the wafer was etched from the back side in TMAH at 90 ^{o}C to stop on the buried oxide to form a diaphragm of around 80 μm by 80 μm area. The nitride was stripped off in boiling phosphoric acid and electron beam lithography was performed on the front to define 100 nm by 100 nm openings with the diaphragm. Next, a short TMAH etch at 60 ^{o}C was performed to etch the SOI, in an inverted pyramid shape, down to the buried oxide. When the buried oxide is removed, a pore of less than 100 nm diameter is formed. A 1000 Å thermal oxide was then grown to shrink the pore to less than 50 nm. Finally, the pore was examined and processed in a transmission electron micrograph and shrunk to the desired nanometer dimension utilizing direct observation. Figure 11 (a) shows the final TEM of the small dimension of a nanopore channel, while figure 11 (b) shows the expected cross-section of the channel with the relevant dimensions at the end of fabrication.

Each nano-pore channel, fabricated according to the process described above, was formed within a die that was 3mm x 3mm in size, and about 0.5mm thick. The die with the nano-pore was sandwiched between two silicone rings and placed in a finely milled pocket within Teflon blocks with the chambers and subsequently clamped, as shown in figure 11 (c). Electrophysiology measurements were performed using an Axon 200B amplifier (Axon Instruments) in the resistive feedback mode, and a CV201 head-stage. To reduce the environmental noise, the nano-pore and the head-stage were placed inside a grounded Faraday cage. The amplifier signal was passed through a 300 Hz low-pass filter (CyberAmp 320) and fed to a Digidata 1322A (Axon Instruments) board on computer with PClamp 9.0 (Axon Instrument) software for data acquisition.

A 200bp fragment from the human CRISP-3 gene (accession number NM_006061) was PCR amplified (forward primer, TCCTGCTGGTAATTGGGCTAA, reverse primer, TGTCCCTGACCAACTGATGTTT) using cDNA from a prostate cancer specimen, and purified by the PCR purification kit (Qiagen, Valencia, CA). The measurements were carried out

in 0.1 M KCl, 2mM Tris (pH 8.5) buffer. To prevent isolation of the nanopore by air bubbles, isopropanol was applied to the exposed surface of the nanopore. Purified DNA at a final concentration of 0.3 μg/ml was applied to one chamber (side 1) and the current measurements from that chamber to the other chamber (side 2) were made. Ag/AgCl electrodes were inserted in the fluid reservoirs and used to make the measurements.

During steady state conditions without DNA, we expect three current components: there will be bulk K^+ and Cl^- currents, $I_{bulk}(K^+)$ and $I_{bulk}(Cl^-)$, and an interfacial layer K^+ current, $I_{int}(K^+)$. We measured steady state ionic currents in the range of 55-70pA through the nanopore channel with 200mV in a 0.1M KCl solution22. (These currents and the dimensions of the channel correspond to resistivity of 81-110Ωcm and these values agreed with our bulk fluid resistivity measurement values of 87Ωcm and theoretical value of 78Ωcm for 0.1M KCl solution. In this calculation, we assume the voltage drop to be across the pore only. The current is expected to flow more through the mobile interface layer due to the higher ionic concentration close to the interface as compared to the bulk layer.) We applied 200bp dsDNA to side 1 and as the dsDNA passed through the pore, it modified the bulk and the interface currents resulting in typical current pulses. However, unexpectedly and in contrast to all the previous reports, we find the signal current to increase rather than decrease during the translocation of dsDNA through the nanopore (see figure 12). (To prove that some DNA molecules have indeed passed through the nanopore, after the experiment, we collected and concentrated the buffers from the two chambers and performed a PCR using the same forward and reverse primers that we used to amplify the DNA. We then ran the PCR products on an ethidium bromide gel and observed a strong band at the expected size from the buffer in side 1. More importantly, we also observed the same size band in the buffer from side 2 proving that some DNA molecules have in fact traveled through the nano-pore from side 1 to side 2). We attribute this surprising increase in current to the following mechanism. As the dsDNA molecule enters the channel, the bulk currents $I_{bulk}(K^+)$ and $I_{bulk}(Cl^-)$ will decrease due to the physical blocking by the DNA molecule, as usually expected. With given channel radius of 2.2nm and dsDNA radius of 1.1nm, we expect the blocking to reduce the current by ~25% (from 75pA to 56pA or $\Delta I_{bulk}(K^+) + \Delta I_{bulk}(Cl^-) \sim -19pA$). However, since the DNA backbone is negatively charged, its translocation will also induce additional K^+ atoms within the channel, and therefore the interface current, $I_{int}(K^+)$, will actually increase. The role of the DNA molecule in this case is analogous to the bottom gate of a double gate field effect transistor that causes the interfacial layer channel charge to increase, resulting in increased current flow due to the voltage applied across the pore. Since the DNA molecule is around the same length as the channel, the current is expected to increase and then decrease as the DNA leaves the pore, as measured.

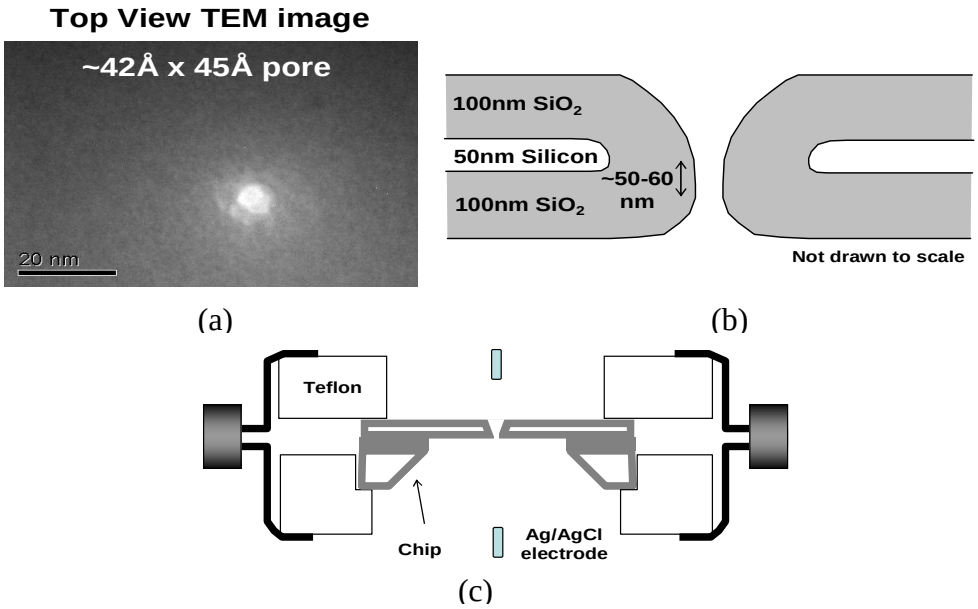

Fig. 11 (a) Transmission electron microscope (TEM) image of the smallest diameter of the nanopore channel in the oxidized silicon membrane. Due to the dimensions shown, the expected channel length is around 50-60nm. (b) Drawn cross-section of the oxidized silicon membrane. (c) Schematic of the apparatus that shows the entire chip within Teflon reservoirs ensuring no fluid leaks across the chambers. The current was measured using Ag/AgCl electrodes. The diaphragm was 80μm x 80μm (Ref. [21]).

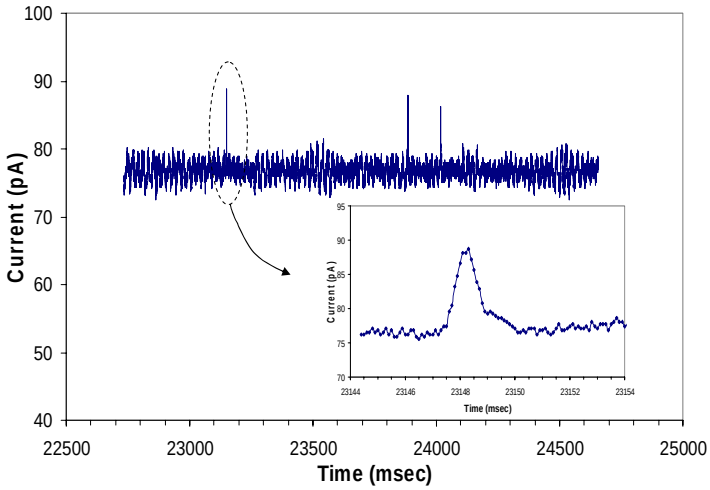

Fig. 12 Translocation of the 200 bp dsDNA molecule. Typical pulses measured for the translocation of the short DNA through the nanopore channel are shown. The inset shows one pulse in more detail (Ref. [21]).

The experimental results presented here demonstrate that the charge on the DNA can be detected in the nanopore channel due to an inherent charge amplification and transduction of the DNA charge into ionic current in the mobile surface charge, similar to a field effect transistor. Clearly, while more detailed experimental work and modeling needs to be performed, including use of longer molecules and improvements in device design such as controlling the interface oxide charge by biasing of the silicon layer, the demonstration of electrical gating effect would allow one to use these nanopore membranes as the third electrode capable of characterizing multiple threads of dsDNA simultaneously. The electrical signal from this device for the passage of short dsDNA molecule with mismatches could exhibit a difference when compared to the signal from matched strands providing a label-free means to detect DNA hybridization. The silicon layer can possibly be used as the third electrode to measure changes in potential during the passage of DNA through the nanopore channel.

6. FUTURE DIRECTIONS AND CONCLUSIONS

Considerable progress has been made in the field of BioMEMS and the research areas now merge and integrate into Nanobiotechnology[23]. The commercial examples of BioMEMS and biochips, including micro-fluidics, continue to rise steadily. Just like MEMS are now considered as the technology to interface the macro world to the nano world, BioMEMS will also enable us to probe, measure, and explore the nano-machinery in the biological world such as single cells and study their function in real-time.

Micro- and nano-scale systems and sensors could allow us to precisely measure the protein, mRNA, and chemical profiles of cells in real time, as a function of controlled stimulus and increase understanding of signaling pathways inside the cell. These are essential to increase our understanding of the underlying cause of basic cell functions such as differentiation, reproduction, apoptosis, etc., and their implications on various disease states. These issues will also be the focus of the post-genomic era and also in the applications of systems theories to biology, also referred to as systems biology[24]. To accomplish these goals, BioMEMS can play an important role, especially in the development of integrated devices and systems for the rapid and real-time analysis of cellular components, especially from single cells. Current expression analysis is performed from an aggregate of cells, lysed at specific time points when the mRNAs are analyzed. The development of microenvironments, as schematically shown in figure 13, where cells can be precisely place, manipulated, lysed, and then analyzed using micro- and nano-sensors in 'real-time', would have a significant impact on systems biology. Integration of sensors for detection of DNA, mRNA, proteins, and other parameters indicating cellular conditions such as oxygen, pH, etc., can be accomplished using BioMEMS platforms and nano-scale sensors. These goals are now being pursued by many groups across the world. Another very exciting research area where novel tools at the micro- and nano-scale can play an important role is in the area of Synthetic Biology, which can be defined as the re-design, fabrication, and alteration of existing biological systems, or design and fabrication of biological systems and sub-systems that do not exist yet[25]. The specific examples of this interdisciplinary field have recently been in the area of

genetically engineering bacterial cells towards the goals of building digital networks. A bacterial oscillator was built using a network of three genes, which was inserted into E. coli cells to form a blinking oscillator[26]. Bacterial genome can be altered using recombinant DNA technology and microorganism can be constructed, potentially, to harness energy, decompose toxic waste, and possibly perform computational functions. As the field progresses, there will be a need for tools and technologies to perform gene insertions into single or very few bacteria, to specifically manipulate their characteristics within a network of bacteria. The tools and platforms to perform such integrated synthetic biology can be provided by BioMEMS and related nano-scale sensors, processing, and device technologies.

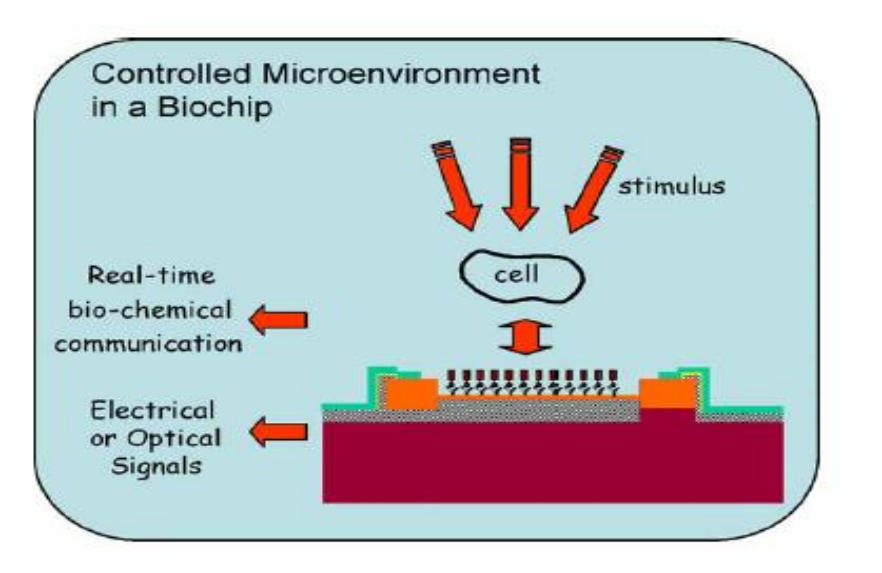

Figure 13. Microfluidic devices with controlled micro-environments for study of cells and the real time profiling of their proteins. mRNA and other biochemicals (Ref. [4]).

Integrated biochips will be very useful in the characterization and detection of microbial cells and microorganisms. In this paper, we reviewed different technologies that can be used to characterize and detect very small numbers of microorganisms in micro-devices. Such electronic/mechanical approaches are very amenable to the realization of portable hand-held devices. The use of dielectrophoresis is very attractive for cell separation and sorting and this function can easily be integrated into micro-fluidic biochips. The metabolic activity of very few bacterial cells confined into a nanoliter volume can be detected using miniaturized impedance microbiology techniques. The metabolic activity of about 50 to 200 live cells can be detected with the current biochip. Silicon based micromechanical sensors can be very sensitive to detection of small masses such as viruses, whose mass ranges in atto-grams. On an even smaller scale, nanopore channels can be used to detect the charge of DNA molecules. All these devices can be coupled with antibody-based recognition, capture and lysing of cells to realize rapid bacterial detection systems, sensitive to a very small number of microorganisms.

ACKNOWLDGEMENT

We would also like to acknowledge the support of the Birck Nanotechnology Center and the staff of the Purdue University Microfabrication facilities for wafer processing. We would also like to acknowledge the support of the NSF Career Award for Rashid Bashir. Haibo Li were supported by the Center for Food Safety Engineering at Purdue University through a USDA cooperative agreement: CRIS 1935-42000-035-00D, agreement # 58-1935-9-010. Hung Chang was supported through NASA Institute of Nanoelectronics and Computing (INAC) at Purdue University under award no. NCC 2-1363. Dr. Demir Akin and Amit Gupta were supported by NIH (NIBIB) grant R21/R33 EB000778-1. The authors would also like to thank Prof. M. Ladisch, Prof. Arun Bhunia, Prof. Steve Broyles of Purdue University, and Dr. Farhad Kosari and Prof. George Vasmatzis of Mayo Clinic, for their collaboration and many valuable discussions.

REFERENCES

1. Mauro Ferrari (Ed.), *Biomedical Nanotechnology, Vol. I-IV*, Kluwer Academic Publishers, 2004, in press.
2. S. Fodor, J. L. Read M. C. Pirrung L. Stryer, A. T. Lu , and D. Solas ,"Light directed spatially addressable parallel chemical synthesis," *Science*, **251**, pp. 767-773, 1991.
3. M. Heller, "An active microelectronics devices for multiplex DNA analysis", *IEEE Engineering in Medicine and Biology*, **15**, pp. 100-103, 1996.
4. R. Bashir, "BioMEMS: state-of-the-art in detection, opportunities and prospects", *Advanced Drug Delivery Reviews"*, **56**, pp. 1565-1586, 2004.
5. H. A. Pohl, "The motion and precipitation of suspensoids in divergent electric fields", *Journal of Applied Physics*, **22**, pp. 869-871, 1951.
6. H. Li, and R. Bashir, "Dielectrophoretic separation and manipulation of live and heat-treated cells of Listeria on microfabricated devices with interdigitated electrodes", *Sensors and Actuators B*, **86**, pp. 215-221, 2002.
7. R. Gómez, R. Bashir, A. K. Bhunia, and M. R. Ladisch, "Microfabricated device for impedance-based detection of bacterial metabolism", Proceedings of the Spring MRS 2002. San Fransisco, CA .
8. D. Akin, H. Li, and R. Bashir, "Real-time virus trapping and fluorescent imaging in microfluidic devices", *Nano Letters*, **4**, pp. 257-259, 2004.
9. Ruth Eden and Gideon Eden, *Impedance Microbiology*, Research Studies Press Ltd., 1984.
10. R. Gomez, R. Bashir, T. Geng, A. Bhunia, M. Ladisch, H. Apple, S. Wereley, "Micro-Fluidic Biochip for Impedance Spectroscopy of Biological Species", *Biomedical Micro-Devices*, **3**, pp. 201-209, 2001.
11. W-J Chang, R. Gomez, H. Li, D. Akin, R. Bashir, "An Investigation of Fluid Absorption in Hybrid Poly(dimethylsiloxane) (PDMS)/Silicon Biochips For Long-term Cell-Incubation Applications", Polymer Materials and Processing for MEMs Technology, American Chemical Society (ACS) Symposium, 2003 Fall National ACS Meeting, New York, September 7-12, 2003.
12. B. Ilic, D. Czaplewski, M. Zalalutdinov, H. G. Craighead, P. Neuzil, C. Campagnolo, and C. Batt, "Single cell detection with micromechanical oscillators", *Journal of Vacuum Science and Technology B*, **19**, pp. 2825-2828, 2001.
13. A. Gupta, D. Akin, and R. Bashir, "Single virus particle mass detection using microresonators with nanoscale thickness", *Applied Physics Letters*, **84**, pp. 1976-1978, 2004.
14. M. A. Cooper, F. N. Dultsev, T. Minson, V. P. Ostanin, C. Abell, and D. Klenerman, "Direct and sensitive detection of a human virus by rupture event scanning", *Nature Biotechnology*, **19**, pp. 833-837, 2001.
15. J. E. Sader, J. W. M. Chon, and P. Mulvaney, "Calibration of rectangular atomic force microscope cantilevers", *Review of Scientific Instruments*, **70**, pp. 3967-3969, 1999.
16. G. F. Bahr, W. D. Foster, D. Peters, and E. H. Zeitler, "Variability of dry mass as a fundamental biological property demonstrated for the case of vaccinia virions", *Biophysical Journal*, **29**, pp. 305-314, 1980.
17. S. Bezrukov, I Vodyanoy, and V. A. Parsegian, "Counting polymers moving through a single ion channel", *Nature*, **370**, pp. 279-281, 1994.
18. J. J. Kasianowicz, E. Brandin, D. Branton, and D. W. Deamer, "Characterization of individual polynucleotide molecules using a membrane channel", *Proceedings of the National Academy of Sciences*, **93**, pp. 13770-13773, 1996.
19. J. Li, D. Stein, C. McMullan, D. Branton, M. J. Aziz, and J. A. Golovchenko, "Ion-beam sculpting at nanometer length scales", *Nature*, **412**, pp. 166-169, 2001.
20. R. Austin, "Nanopores: The art of sucking spaghetti", *Nature Materials*, **2**, pp. 567-568, 2003.
21. H. Chang, F. Kosari, G. Andreadakis, M. A. Alam, G. Vasmatzis, and R. Bashir, "DNA-Mediated fluctuations in ionic currents through silicon oxide nanopore channels", *NanoLetters*, **4**, pp. 1551-1556, 2004.
22. A. J. Storm, J. H. Chen, X. S. Ling, G, H. W. Zandbergen and C. Dekker, "Fabrication of solid-state nanopores with single-nanometer precision**"**, *Nature Materials*, **2**, pp. 537-540, 2003.
23. G.M. Whitesides, "The right size in nanobiotechnology", Nature Biotechnology, **21**, pp. 1161– 1165, 2003.
24. L. Hood, D. Galas, "The digital code of DNA", *Nature*, **421**, pp. 444– 448, 2003.
25. D. Ferber, *Science*, **303**, pp.158-161, 2004.
26. M.B. Elowitz, S. Leibler, "A synthetic oscillatory network of transcriptional regulators", *Nature*, **403**, pp. 335–338, 2000.